The Use of High-Resolution Imagery for Identification of Urban Climax Forest Species Using Traditional and Rule-Based Classification Approach

Ramanathan Sugumaran, Manoj Kumar Pavuluri, *Student Member, IEEE*, and Daniel Zerr

***Abstract*—Columbia, MO, is one of the fastest growing cities in the United States. The rapid urbanization is jeopardizing the city's urban climax forests, which are defined as any woodland community of more than 7.53 ha dominated by plant species such as oak and hickory. The increasing urban pressure places heavy demands on city planners to seek better management approaches to ensure that these plant species, which are native to Missouri, are protected even when threatened by new developments. Traditionally, planners are identifying these areas by surveys, which are costly, time consuming, and conducted on an as-needed basis. The current study is to test the feasibility of high-resolution satellite and airborne imagery for the identification of these forests and to assist planners in preserving them. In order to identify these climax forests, 4-m multispectral IKONOS images for April and August 2000 and 25-cm and 1-m multispectral airborne photographs for September and November 2001 were acquired and used in this study. These images were classified using a traditional classifier [maximum likelihood (ML)] and a rule-based classifier [classification and regression tree (CART)]. Results show that the images taken in September using the ML classifier are more useful in identifying the tree species in the study area. Among the spatial resolutions used, 1-m images proved to be optimal in recognizing trees and at the same time minimizing shadows.**

***Index Terms*—Classification, classification and regression tree (CART), multitemporal satellite imagery, plant identification.**

I. INTRODUCTION

THE LAND COVER products required for better management, maintenance, and conservation by the planning department of the city of Columbia, MO, include a green belt map and climax forest map. A climax forest is a woodland community of over 7.53 ha, dominated by climax species such as oak and/or hickory. Knowledge about the identification and extent of these forests within the Columbia metropolitan area is valuable to the planning department for issuing building permits, since these trees constitute native forest in Missouri and need to be protected. Presently, these patches are identified by fieldwork, which is very costly and time consuming. We made an attempt to develop a methodology to produce a potential climax forest map for the city of Columbia metro area using high spatial resolution satellite images and airborne images for different seasons. Previous studies in this area used coarse spatial resolution images like Landsat Enhanced Thematic Mapper (ETM) and tested them with maximum likelihood (ML) and other traditional classifiers for general vegetation mapping [1].

Several researchers have worked on classifying forest vegetation using different sensors, spatial resolution (measure of the smallest object that can be resolved by the sensor) and spectral resolution (the number of spectral bands imaged by the sensor) for different purposes with airborne and satellite platforms. For example, moderate spatial resolution satellite images such as Landsat Thematic Mapper (TM), SPOT, and Indian Remote Sensing for mapping, quantifying, and monitoring changes in the physical characteristics of forest cover has been widely reported [2], [3]. They all suggested that forest vegetation mapping required higher spatial and spectral resolution. Lately, several researchers have started using higher spatial resolution images for tree species identification. Gougeon [3] compared the individual tree crown recognition from aerial photographs with different spatial resolution satellite images. He suggests that images with 1-m resolutions are more useful for tree crown recognition than images with higher spatial resolution. In another study [4], Gougeon used high-resolution images covering large areas for forest regeneration using the traditional classifiers such as ML. Zhang [5] discusses the difficulties of identifying trees in urban environments and proposes a method to extract information from high-resolution images using not only the spectral data but also the spatial properties. For example, Biging *et al.* [6] and Ramsey *et al.* [7] used images with pixel size of 0.5 m for assigning tree crowns. Cohen *et al.* [8] tried classification of conifer canopies using images with a spatial resolution, finer than 1 m. Skidmore [9] used an expert classifier system for classifying eucalyptus trees using Landsat data. Rule-based classification using *classification and regression trees* (CART) was used recently to identify some tree species using additional data such as digital elevation model (DEM) and soil properties. Most of the studies used either a single-season single spatial resolution or a single classifier for the identification of tree species as in [10] and [11]. Several researchers [12]–[14] showed good results using CART as a rule-based classifier for land cover mapping. In

Manuscript received September 13, 2002; revised May 26, 2003. This work was supported by the National Aeronautics and Space Administration and the Raytheon/STX Corporation under Subcontract 012100MJ-3.

R. Sugumaran is with the Department of Geography, University of Northern Iowa, Cedar Falls, IA 50614-0406 USA (e-mail: sugu@uni.edu).

M. K. Pavuluri and D. Zerr are with Center for Agriculture, Resource and Environmental Systems, University of Missouri, Columbia, MO 65211 USA.

Digital Object Identifier 10.1109/TGRS.2003.815384

TABLE I

Sensor	Spatial resolution	Spectral resolution	Radiometric Resolution	Collection Azimuth (In degrees)	Collection Elevation (In degrees)	Sun Angle Azimuth (In degrees)	Sun Angle Elevation (In degrees)
IKONOS Multispectral April, 2000	4m	4bands Blue, green, red, NIR	11-bit	99.9	52.6	131.2	54.4
IKONOS Multispectral Aug, 2000	4m	4bands Blue, green, red, NIR	11-bit	343.4	68.9	153.1	50.1
IKONOS Panchromatic April 2000	1m	1band (0.45 - 0.90 microns)	11-bit	99.9	52.6	131.2	54.4
Airborne Nov, Sep 2001	1m	4bands	8-bit	-	-	-	-
Airborne Nov 2001	25cm	4bands	8-bit	-	-	-	-
Soil	30m	na	8-bit	-	-	-	-

this study, we tried to compare the results of images with varying spatial resolution taken at different times of the year and classifying them using traditional and rule-based classifiers. In addition, we also tried to examine the problems faced with shadow pixels in high spatial resolution images and to identify some measures to overcome them.

II. Materials and Methods

A. Study Area

In order to test the methodology a small test site within the campus area of University of Missouri—Columbia, MO, was selected. The reason for selecting this study area is because information on the characteristics and location of tree species was readily available from the University Landscape services on the campus. It covers an area of 41.4 ha and contains eight different species of oak and many other species of trees. The major kind of oak in this area is pin oak (*Quercus palustris*). The others are red oak (*Quercus rubra*), swamp white oak (*Quercus bicolor*), willow oak (*Quercus phellos*), black oak (*Quercus kelloggii*), shingle oak (*Quercus imbricaria*), chinkapin oak (*Quercus muehlenbergii*), and schumard oak (*Quercus schumardii*). Although the study site is small the methods discussed here can be applied to larger areas if data are available. Taking a small area solved the problems inherent to mosaicing images for large-area coverage. Such techniques may affect the overall classification if the area is large with various types of land cover having overlapping spectral regions. In addition, most of the area is flat with no or negligible variation in elevation.

B. Data Used

Available images for this study are IKONOS multispectral and panchromatic images for two seasons and airborne orthorectified images. The details are given in Table I. Previous researchers used satellite images for plant species identification with some ancillary data for achieving higher accuracy [14], [15]. In addition, soil, DEM, and slope information were used as ancillary data to aid in the CART classification. The main focus of the study was to make efficient use of the spectral data available in different seasons (August, April, September, November) with different resolutions (25 cm, 1 m, 4 m) and with different classifiers (ML and CART).

The availability of images with varying spatial resolutions raised several issues and practical problems in selecting appropriate image(s). The ideal pixel size depends on the size of tree crowns, which is highly variable both within, as well as between species [16]. Here some of the problems are discussed along with the methods to resolve them. Images with higher spatial resolution are more useful in identifying different objects on the ground [17]. High spatial resolution generally implies limited spectral and temporal resolution. The choice of spatial resolution needed for the purpose of this study was discussed in [18]. Here, we need to distinguish between different trees that have varying crown diameters, which make the task even more complicated. So, 1-m images would be a better choice than 4-m IKONOS images for this application mainly because of better spatial resolution to identify trees crowns. However, both one meter and four meter images have various problems such as direction of shadow, length of shadow, percentage of the tree in shade, etc. These problems are discussed in the training data and result sections.

C. Image Analysis

1) Preprocessing: Two IKONOS (4 m) and two airborne (1 m) images were imported into ERDAS Imagine software with UTM projection, Zone 15 in NAD83 datum. In this study, the 4-m IKONOS image was spatially enhanced to a 1-m image using the panchromatic layer to maintain the consistency that all images used for the study are of 1 m. Several studies have shown the advantages of enhancing the spatial resolution of multispectral images [19]. Some of the popular methods in resolution merging are intensity hue saturation (IHS) [20], inverse principal component analysis (PCA) [21], highpass filter (HPF) [22], Brovey transform, color-normalized [19], and wavelet transform [23]. Several researchers had evaluated and compared these methods. principal component (PC) and IHS methods are more dependent on the spectral overlap of the original data. The PC method gives better results regarding the reproduction of spatial information.[1] In this study, we applied the principal component rule for the resolution merge and cubic convolution technique to resample the multispectral input to that of the high-resolution panchromatic image using the option available within ERDAS Imagine software. As the August panchromatic image was not available (Table I), only the April image was enhanced. Along with these images, 1-m airborne images for the same area were also used for classification.

2) Training Data: The pixel samples from a point (usually the top) of the canopy could be used to represent the canopy as a whole [24]. Therefore, the training data collected were only from the crowns of the trees. As pin oak is dominant in the study area we focused our study on the identification of this trees species only. The spectral response for pin oak was taken from a sun-lit part of a crown and used as a reference signature. In this way 20 training sets were collected from different oak trees. This was verified with the ground truth data. Trees are seen with only a portion of the crown exposed to light with a major portion in shade. This leads to overlapped spectral space of the shadows of tree leaves inside the trees and the shadows of urban features. Spectral values for the same trees taken in different months vary drastically. These changes also aid in differentiating the species. In this way the signatures for all the classes are noted and the image that has highest variance between the classes is considered to be most useful in distinguishing the species.

The pixels for training data selected from the imagery are from the portions of the tree, which are completely exposed to sunlight. Shadow pixels inside the tree crown were avoided. These are the shadows of leaves and smaller branches in the tree. As the spatial resolution increases the shadow pixels in-between the leaves become more prominent. Shadowed portions of all the trees are classified into a separate class. The task of classifying the shadow pixels of different trees into different classes becomes even more complex. For this study, all the shadow pixels of all the trees are classified into one class. The details of this are discussed in the methodology section.

3) Classification: The main objective of the study is to differentiate urban climax forest species such as oak species from other trees present in the study area using different spatial resolutions, seasons and different classification algorithms. The study area is dominated by pin oak amongst the oak species. All the images available were classified separately using the same training data. Classification was done using the ML method, a parametric classification algorithm and CART, which is a nonparametric algorithm. The flowchart for this procedure is shown in Fig. 1.

ML classification is based on different factors such as the nature of the distribution and probabilities of the classes chosen. The distribution needs to be normal Gaussian distribution. Considering the Mahalanobis distance measure the classifier would be in the form below

$$L_k(X) = \frac{1}{(2\pi)^{\frac{1}{2}}|S_k|^{\frac{1}{2}}} \exp\left\{-\frac{1}{2}(X-\overline{X_k})^T {S_k}^{-1}(X-\overline{X_k})\right\}$$

where L_k is the likelihood estimator, S_k is the covariance matrix and X_k is the mean vector. This algorithm is more efficient in

[1]Infoterra. See http://www.infoterraglobal.com/explore/bands.htm.

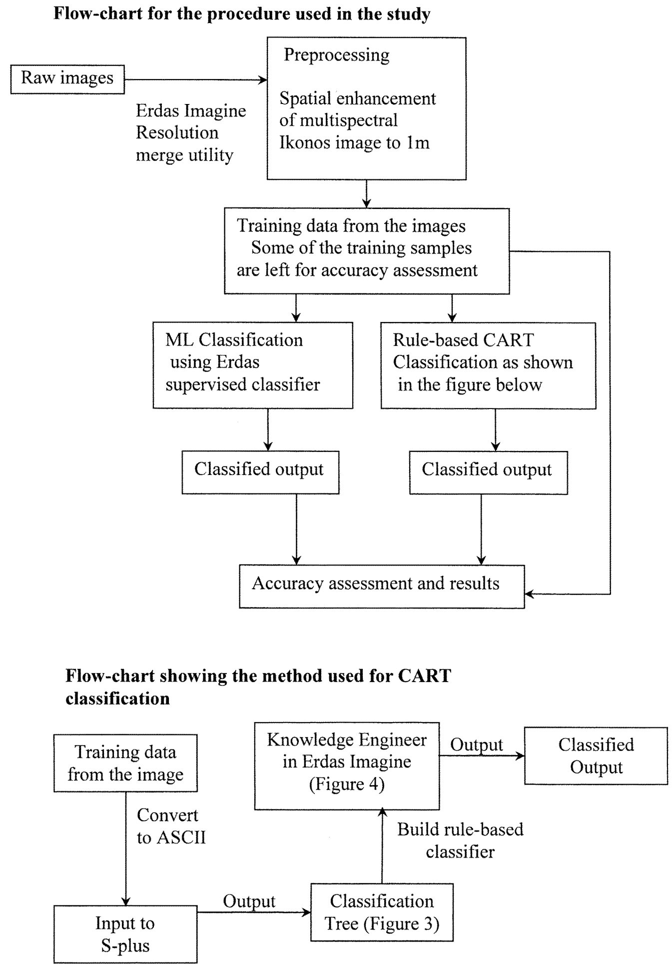

Fig. 1. Flowchart showing the methodology used and CART classification.

use if the mean of all the training sets collected for a class are the same or close [25].

Traditional classifiers such as ML purely rely on the spectral information. In this study, we combined spectral values and ancillary data for the classification of climax forest species using a rule-based classification with a popular statistical technique known as CART. A rule-based classification requires expert knowledge [14]. In this case we used CART algorithm to achieve that information. CART is a term coined by Breiman [26], where he describes various algorithms for splitting, construction and pruning decision trees. Lately, this algorithm has been implemented in statistical software such as S-PLUS. CART is a recursive-partitioning algorithm and identifies the splitting variables based on an exhaustive search of all possibilities. Several splitting algorithms are used in CART, of which the Gini index of diversity is used for this study [26]. The Gini index is calculated as follows.

- Let n_i = number of observations in class i; let $P_i = n_i/n$ and $P_j = n_j/n$.
- n_j = number of observations in class j.
- n = number of total observations in the dataset.

Gini index is an impurity function defined as

$$g(t) = \sum_{i \neq j} p_i \cdot p_j$$

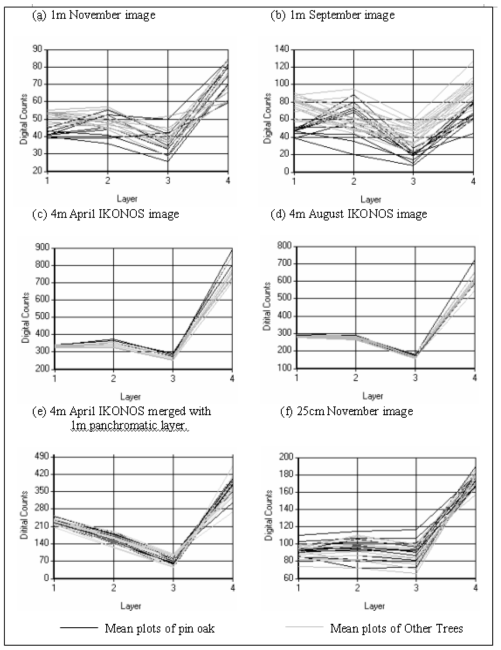

Fig. 2. Spectral response comparison in different images. It shows the plots of digital counts for the four layers: blue, green, red, and infrared. The layers in the figure represent the four bands of the image. The figure also shows that these values have a higher range for all the IKONOS images and lesser for the airborne images. This is because airborne images are eight-bit images (0–255) and IKONOS (0–2048) are 11-bit images.

which can also be written as

$$g(t) = \left(\sum_j p_j\right)^2 - \sum_j {p_j}^2 = 1 - \sum_j {p_j}^2$$

at a point given t.

Here t is a point in the dataset where the current split occurs. It can be interpreted as the estimated probability of misclassification. Different forms of this rule can be interpreted differently according to the user. This is discussed in detail in [26] and presented in different forms.

The following section describes the splitting.

1) The Gini index is computed for every value of all the features in the dataset for the first iteration. Here features are the four bands present in the image.
2) Wherever the index is least, the data are split at that point and at that feature.
3) Once the data are split using a specific criterion (usually greater than or less than), the Gini index is computed for all the features and at only those points that are inside the split boundaries.
4) Every split gives two *subtrees* (left and right) and the split forms a node.
5) Again wherever it is least in both the sides of the split, it is used for the next iteration. This continues until a stopping condition is reached. Stopping conditions may use a threshold for the Gini index at a node, or it can be the depth of the tree at the node. Stopping conditions can be changed based on the data and the application of the tree.

It works efficiently with data that are non-Gaussian on highly skewed and multimodal data. This makes it more suitable for the current dataset in the study, as the spatial resolution is high; the training data tend to become more heterogeneous. This is evident from the figures showing the mean plot of all the classes in Fig. 2. The data need not be of a normal distribution. For CART classification, using the training data collected, the classification tree was built using S-plus software [Fig. 3(a) and (b)]. Each path from the root node to the leaf gives a rule for the class represented by the leaf node. These rules are then used to build the rule-based classifier with knowledge engineer provided in Erdas Imagine software (Fig. 4). The tree generated in the above procedure uses only the spectral values of the image.

Another method was tried to reduce the effect of shadow pixels inside the trees. The raw image was smoothed using a 7×7 window to suppress shadow effects within the crown. Along with this a texture image with a 5×5 window was used to delineate the crown boundaries. Due to the high variability of the size of the crowns in the study area this did not give the anticipated results. Since such a method would change the pixel values of the image, it cannot be used for applications, which deal with the calculation of the area for classification and not distinct objects [27]. This method groups the pixels of similar values. It isolates the tree pixels into a group from the shadow pixels. This can be more useful in getting a homogeneous signature from a particular tree.

4) Accuracy Assessment: The normal procedures for accuracy measurements are based on the number of pixels classified correctly. In our study the number of trees crowns classified correctly determines the accuracy. The shaded portions of the tree are classified into shadows. The trees counted here are based on the crown cover. If the majority of the crown pixels are classified into a class, the tree is counted for that class (Table III). This gives a measure of the classifier accuracy. Researchers in a study used a similar approach to identify Chinese willow trees [6]. The concentration here is only on how well the single trees are picked up by the classifier, not on the area classified.

III. Results and Discussion

The results obtained using different classifiers and different spatial resolution imagery acquired at different times of the year are shown in Fig. 5. Airborne images taken in September with 1-m resolution proved to be useful in identifying the oak species. The classification using the ML method using each training set as an individual class showed considerable improvement in the results. These are discussed individually in the subsequent sections.

The classification output differs for ML and CART. As discussed earlier, due to the shadow pixels and high resolution of the images there is very high variation even in a small training set. This made the signatures for the same class highly heterogeneous. This leads to misclassification when using ML because the data are no longer a Gaussian distribution. These types of data are more suitable for classification using CART than ML. The classified output of ML and CART do not show much variation in identification of oak trees from others (Fig. 5). They do, however, vary in the classification of other land cover classes. Misclassification of land cover such as grass and other trees is less in CART [Fig. 5(e)–(h)], but the major difference is in the

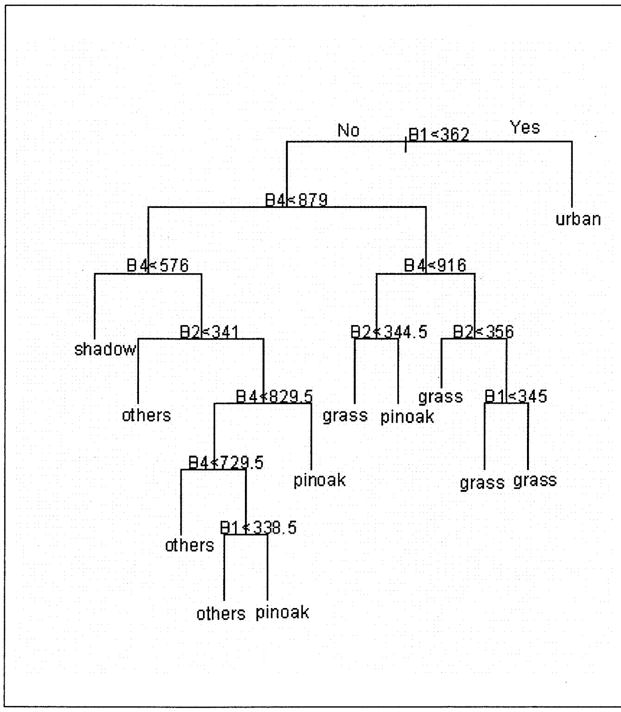

(a)

```
*** Tree Model ***
Classification tree:
Variables actually used in tree construction:
 "B1" "B4" "B2"
Number of terminal nodes:  12
Misclassification error rate: 0.02263 = 11 / 486
node), split, n, deviance, yval, (yprob)  * denotes terminal node

 1) Root 486 1257.000 urban ( 0.2078 0.10910 0.03498 0.1317 0.5165 )
  2) B1<362 235 584.200 grass ( 0.4298 0.22550 0.07234 0.2723 0.0000 )
    4) B4<879 124 228.900 shadow ( 0.0000 0.39520 0.08871 0.5161 0.0000 )
      8) B4<576 65   10.330 shadow ( 0.0000 0.01538 0.00000 0.9846 0.0000 ) *
      9) B4>576 59   56.760 others ( 0.0000 0.81360 0.18640 0.0000 0.0000 )
       18) B2<341 31    0.000 others ( 0.0000 1.00000 0.00000 0.0000 0.0000 ) *
       19) B2>341 28   37.520 others ( 0.0000 0.60710 0.39290 0.0000 0.0000 )
         38) B4<829.5 23   26.400 others ( 0.0000 0.73910 0.26090 0.0000 0.0000 )
           76) B4<729.5 7    0.000 others ( 0.0000 1.00000 0.00000 0.0000 0.0000 ) *
           77) B4>729.5 16   21.170 others ( 0.0000 0.62500 0.37500 0.0000 0.0000 )
            154) B1<338.5 10   10.010 others ( 0.0000 0.80000 0.20000 0.0000 0.0000 ) *
            155) B1>338.5 6    7.638 pinoak ( 0.0000 0.33330 0.66670 0.0000 0.0000 ) *
         39) B4>829.5 5    0.000 pinoak ( 0.0000 0.00000 1.00000 0.0000 0.0000 ) *
    5) B4>879 111   80.670 grass ( 0.9099 0.03604 0.05405 0.0000 0.0000 )
     10) B4<916 17   34.600 grass ( 0.5294 0.23530 0.23530 0.0000 0.0000 )
       20) B2<344.5 10    6.502 grass ( 0.9000 0.10000 0.00000 0.0000 0.0000 ) *
       21) B2>344.5 7    9.561 pinoak ( 0.0000 0.42860 0.57140 0.0000 0.0000 ) *
     11) B4>916 94   19.360 grass ( 0.9787 0.00000 0.02128 0.0000 0.0000 )
       22) B2<356 65    0.000 grass ( 1.0000 0.00000 0.00000 0.0000 0.0000 ) *
       23) B2>356 29   14.560 grass ( 0.9310 0.00000 0.06897 0.0000 0.0000 )
         46) B1<345 9    9.535 grass ( 0.7778 0.00000 0.22220 0.0000 0.0000 ) *
         47) B1>345 20    0.000 grass ( 1.0000 0.00000 0.00000 0.0000 0.0000 ) *
  3) B1>362 251    0.000 urban ( 0.0000 0.00000 0.00000 0.0000 1.0000 ) *
```

(b)

Fig. 3. (a) Decision-tree obtained from CART, using S-plus software for the IKONOS April 4-m data. Each node represents a decision condition. All the leaf nodes represent class variables. Each class can be have more than one leaf node. Every leaf node has a unique path from the root, which forms a decision rule for that class, e.g., a rule for pin oak class can be derived as follows. Let B1, B2, B3, and B4 represent the four bands of image if (B1 $<$ 362 and B4 $\Rightarrow$ 879 and B4 $<$ 916 and B2 $\Rightarrow$ 344.5) then Class $=$ Pin oak. (b) The iterations in the tree construction. The numbers used as index are the node values which are computed as follows. If the root node is n, then left and right child nodes are numbered $2n$ and $2n+1$, respectively. The values indicated by bold letters represent the highest probability among all the classes. Nodes ending with "$*$" are the leaf nodes.

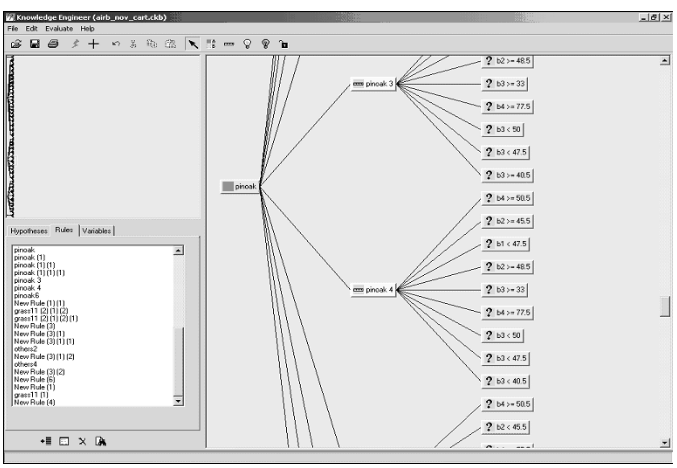

Fig. 4. Part of the rule-based classifier constructed using Erdas Imagine Knowledge engineer. These rules are derived from the decision tree obtained from the S-plus software.

unclassified pixels. There are no unclassified pixels from the ML method, whereas CART leaves many pixels unclassified. This is because the CART classification here is a rule-based classification and the pixel values that do not fall in any of the specified rules for all the classes are left unclassified. ML is a distance-based classifier and every pixel is assigned to class mean value closest to it. In CART classification, all the unclassified pixels were from the shadow class as identified by the ML classification.

In the images with 1-m resolution, the tree crowns could be identified with a minimum shadow effect. In the 25-cm images the trees are seen more clearly but as the resolution is so high the number of shadow pixels also increases. In 4-m images, the tree crowns cannot be separated from their shadows as it spans only one or two pixels. Therefore, the 4-m images were not included in the accuracy comparison in Tables II and III.

Seasonally, the September image proved to be most useful. This is evident from the fact that it was acquired at the time of fall colors. Among all the spectral bands, the blue band had a better separation of oak reflectance values from other tree species. The reason for better separation of the oak species in autumn is due to changes in amount of chlorophyll pigmentation [28]. Using the blue band proved helpful in the identification of tree species in a previous study [17], [23]. The effect of fall foliage can be observed in the September airborne image where the spectral distinction in the blue band is prominently seen [Fig. 5(b)]. The airborne images have considerable distinction in the blue bands. The overlap in spectral space of all the bands, as seen in Fig. 5(c)–(e), explains the misclassification of the trees. The other possible reasons for the misclassifications with this data may be due to the improper lighting conditions during image acquisition and differences in shadow directions and length in different images.

There are several factors affecting the species classification. Differences within the species may be due to the variations in the use of chemicals used for fertilizing the tree [29], reflectance of the canopy [30], [31], climatic differences [32], soil charac-

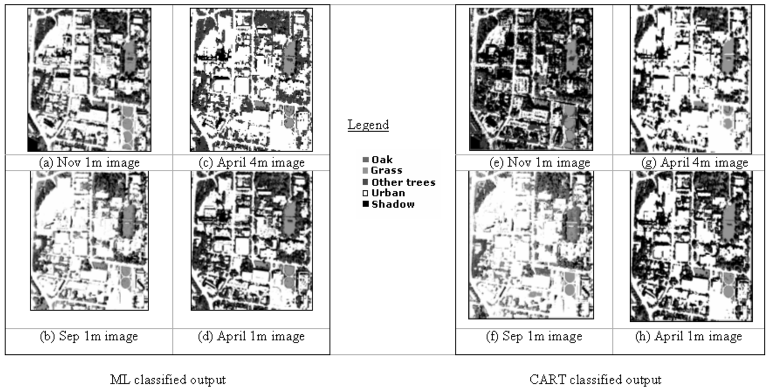

Fig. 5. Classified output of different images in the study area.

TABLE II
CART CLASSIFICATION

Images	*Oak: total 47*	*Other trees: total 540*	*Oak %*	*Others %*
Nov airborne	21	532	44.6	98.5
Sep airborne	37	522	78.7	96.6
April IKONOS (enhanced)	44	464	93.6	85.9

TABLE III
ML CLASSIFICATION

Images	*Oak: total 47*	*Other trees: total 540*	*Oak %*	*Others %*
Nov airborne	18	519	38.2	96.1
Sep airborne	41	533	87.2	97.8
April IKONOS (enhanced)	42	486	89.3	90.0

teristics, precipitation, topography, multiple reflections within the canopy [33], and the soil background and many other environmental factors [34]. Variance within a single tree may be due to age differences between leaves within the crown [35]. The future study will use sensitivity analysis to analyze which factor has the strongest influence on the results.

IV. CONCLUSION AND FUTURE DIRECTIONS

In this study, we compared the results of classifications of images with varying spatial resolution taken at different times of the year and classifying them using traditional and rule-based classifiers. Combinations of different multispectral images provide a lot of information for species classification. From the results of images from four seasons, it was found that the images taken in September are the most useful in identification of tree species. Comparisons of spatial resolutions showed that 1-m resolution is optimal for reducing the shadow effects in-between the trees. This methodology can be applied to larger areas, which would help in the identification of tree species in urban areas.

With the current spatial resolution and high spectral resolution, it will be possible to trace every tree and detect within-species and between-species variations. The future directions will include the use of hyperspectral images with a good spatial resolution for tree species classification and sensitivity analysis for the identification of major factors that influence the results. When dealing with small areas with larger number of species to be identified, hyperspectral images would be a better choice. If the area of study is very large the size and cost of hyperspectral images needed for it is not favorable for computation and is not cost efficient. This trade-off between better spectral and spatial resolutions should be considered according to the purpose of the study.

ACKNOWLEDGMENT

The authors wish to thank J. Fleck and S. Vale of the city of Columbia, MO, for their ideas and cooperation in this work.

REFERENCES

[1] R. Sugumaran, D. Zerr, and T. Prato, "Multi-temporal IKNONS images for local government planning and management," *Can. J. Remote Sens.*, vol. 28, no. 1, pp. 90–95, 2002.
[2] R. Nemani and S. W. Running, "Implementation of a hierarchical global vegetation classification in ecosystem function models," *J. Veg. Sci.*, vol. 7, no. 3, pp. 337–346, 1996.

[3] F. A. Gougeon, "Towards semi-automatic forest inventories using individual tree crown (ITC) recognition," Forestry Res. Applications, Pacific Forestry Centre, Tech. Rep., 2000.

[4] ——, Recognizing the forest from the trees: Individual tree crown delineation, classification and regrouping for inventory purposes. presented at 3rd Int. Airborne Remote Sensing Conf. and Exhibition. July 7–10, 1997.

[5] Y. Zhang, "A spectral and spatial information integrated approach for tree extraction from high-resolution digital imagery," in *Proc. Digital Earth 2001*. Fredericton, NB, Canada: Can. Inst. Geomatics, June 24–28.

[6] G. S. Biging, M. Dobbertin, and E. C. Murphy, "A test of airborne multispectral videography for assessing the accuracy of wildlife habitat maps," *Can. J. Remote Sens.*, vol. 21, pp. 357–366, 1995.

[7] E. W. Ramsey III, G. A. Nelson, S. K. Sapkota, E. B. Seeger, and K. D. Martella, "Mapping chinese tallow with color-infrared photography," *Photogramm. Eng. Remote Sens.*, vol. 68, pp. 251–255, 2002.

[8] W. B. Cohen, T. A. Spies, and G. A. Bradshaw, "Semivariograms of digital imagery for analysis of conifer canopy structure," *Remote Sens. Environ.*, vol. 34, pp. 167–178, 1990.

[9] A. J. Skidmore, "An expert system classifies eucalypt forests types using thematic mapper data and a digital terrain model," *Photogramm. Eng. Remote Sens.*, vol. 55, pp. 1449–1464, 1989.

[10] K. R. Harvey and G. J. E. Hill, "Vegetation mapping of a tropical freshwater swamp in the northern territory, Australia: A comparison of aerial photography, Landsat TM and SPOT satellite imagery," *Int. J. Remote Sens.*, vol. 22, pp. 2911–2925, 2000.

[11] C. E. Woodcock, J. B. Collins, S. Gopal, V. D. Jakabhazy, X. Li, S. Macomber, S. Ryherd, V. Harward, J. D. Levitan, Y. Wu, and R. Warbington, "Mapping forest vegetation using Landsat TM imagery and a forest reflectance model," *Remote Sens. Environ.*, vol. 50, pp. 240–254, 1994.

[12] R. S. De Fries, M. Hansen, J. R. G. Townshend, and R. Sohlberg, "Global land cover classification at 8 km spatial resolution: The use of training data derived from Landsat imagery in decision tree classifiers," *Int. J. Remote Sens.*, vol. 19, pp. 3141–3168, 1998.

[13] G. Gerylo, R. J. Hall, S. E. Franklin, A. Roberts, and E. J. Milton, "Hierarchical image classification and extraction of forest species composition and crown closure from airborne multispectral video imagery," *Can. J. Remote Sens.*, vol. 24, pp. 219–232, 1998.

[14] R. L. Lawrence and A. Wright, "Rule-based classification systems using Classification and Regression Tree (CART) analysis," *Photogramm. Eng. Remote Sens.*, vol. 67, pp. 1137–1142, 2001.

[15] W. Bingfang, H. Xuan, and T. Zhigang, "Vegetation mapping using remote sensing and GIS," *J. Chinese Geograph.*, vol. 4, pp. 112–123, 1994.

[16] H. Nagendra, "Using remote sensing to assess biodiversity," *Int. J. Remote Sens.*, vol. 22, pp. 2377–2400, 2001.

[17] P. Meyer, K. Staenz, and K. I. Itten, "Semi-automated procedures for tree species identification in high spatial resolution data from digitized color infrared-aerial photography," *ISPRS J. Photogramm. Remote Sens.*, vol. 51, pp. 5–16, 1996.

[18] T. Key, T. A. Warner, J. B. McGraw, and M. A. Fajvan, "A comparison of multispectral and multitemporal information in high spatial resolution imagery for classification of individual tree species in a temperate Hardwood forest," *Remote Sens. Environ.*, vol. 75, pp. 100–112, 2001.

[19] J. Vrabel, "Multispectral imagery band sharpening study," *Photogramm. Eng. Remote Sens.*, vol. 62, pp. 1075–1083, 1996.

[20] A. K. Saraf, "IRS-1C-LISS-III and PAN data fusion: An approach to improve remote sensing based mapping techniques," *Int. J. Remote Sens.*, vol. 20, no. 10, pp. 1929–1934, July 1999.

[21] D. L. Civco and J. D. Hurd, "A hierarchical approach to land use and land cover mapping using multiple image types," in *Proc. 1999 Annu. ASPRS/ASCM Convention* Portland, OR, pp. 687–698.

[22] P. S. Chavez and J. A. Bowell, "Comparison of the spectral information content of landsat thematic mapper and SPOT for three different sites in the phoenix, arizona region," *Photogramm. Eng. Remote Sens.*, vol. 54, no. 12, pp. 1699–1708, 1988.

[23] H. Li, B. Manjunath, and S. Mitra, "Multisensor image fusion using the wavelet transform," *Graph. Models Image Process.*, vol. 57, no. 3, pp. 235–245, 1995.

[24] S. J. Gill, S. B. Gregory, and E. C. Murphy, "Modeling conifer tree crown radius and estimating canopy cover," *Forest Ecol. Management*, vol. 126, pp. 405–416, 2000.

[25] M. Netzband, G. Meinel, and R. Lippold, "Classification of settlement structures using morphological and spectral features in fused high resolution satellite images (IRS-1c)," *Int. Arch. Photogramm. Remote Sens.*, vol. 32, no. 7-4-3 W6, June 1999.

[26] L. Breiman, F. Jerome, O. Richard, and S. Charles, *Classification and Regression Trees*. Belmont, CA: Wadsworth Int. Group, 1984.

[27] *Erdas Imagine Field Guide*, 4th ed. Atlanta, GA: ERDAS, 1997.

[28] N. M. A. Daley, C. Burnett, M. Wulder, K. O. Niemann, and D. G. Goodenough, "Comparison of fixed-size and variable size windows for the estimation of tree crown position," in *Proc. IGARSS*, Seattle, WA, July 6–10, 1998.

[29] V. Demarez, E. J. P. Gastellu, E. Mougin, G. Marty, C. Proisy, E. Dufrene, and V. Le Dantec, "Seasonal variation of leaf chlorophyll content of a temperate forest. Inversion of the PROSPECT model," *Int. J. Remote Sens.*, vol. 20, pp. 879–894, 1999.

[30] Y. Inoue and M. S. Moran, "A simplified method for remote sensing of daily canopy transpiration—a case study with direct measurements of canopy transpiration in soybean canopies," *Int. J. Remote Sens.*, vol. 18, pp. 139–152, 1997.

[31] M. M. Lewis, "Species composition related to spectral classification in Australian spinifex hummock grassland," *Int. J. Remote Sens.*, vol. 15, pp. 3223–3239, 1994.

[32] T. Key, T. A. Warner, J. B. McGraw, and M. A. Fajvan, "An evaluation of the relative spectral and phenological information for tree canopy classification of digital images in the eastern deciduous forest," in *Presentation in the Int. Forum on Automated Interpretation of High Spatial Resolution Digital Imagery for Forestry*, Victoria, BC, Canada, Feb. 10–12, 1998, pp. 243–254.

[33] G. A. Blackburn and E. J. Milton, "Seasonal variations in the spectral reflectance of deciduous tree canopies," *Int. J. Remote Sens.*, vol. 16, pp. 709–720, 1995.

[34] A. R. Huete, R. D. Jackson, and D. F. Post, "Spectral response of a plant canopy with different soil backgrounds," *Remote Sens. Environ.*, vol. 17, pp. 37–53, 1985.

[35] D. A. Roberts, M. O. Smith, and J. B. Adams, "Green vegetation, nonphotosynthetic vegetation, and soils in AVIRIS data," *Remote Sens. Environ.*, vol. 44, pp. 255–269, 1993.

Ramanathan Sugumaran received the Ph.D. degree in geography from the University of Edinburgh, Edinburgh, U.K.

He is currently an Assistant Professor of geography at the University of Northern Iowa, Cedar Fall, and an affiliated faculty member in the Center for Agricultural, Resource and Environmental Systems, University of Missouri—Columbia, Columbia. He is currently teaching introductory GIS, advanced GIS, remote sensing of the environment, digital image processing, and global positioning systems. He has received research grants from NASA, Raytheon Corporation, Midwest Transportation Consortium, NOAA, the Iowa Space Consortium, and the Missouri DNR. He has over 12 years of research experience in remote sensing applications, spatial analysis using GIS, decision support systems for natural resource management, artificial intelligence applications, and Internet-based GIS modeling. He has published several refereed journal articles in remote sensing, GIS, decision support systems, and artificial intelligence-related journals.

Manoj Kumar Pavuluri (S'02) received the B.E. degree in computer science from Kakatiya University, Khammam, India, in 2000. He is currently pursuing the M.S. degree in computer science at the University of Missouri, Columbia.

He is a Research Assistant in the Center for Agriculture, Resource, and Environmental Systems (CARES), University of Missouri, Columbia. His research interests include developing methodologies for improving classification accuracy of satellite images and Internet mapping services.

Daniel Zerr received the B.S. degree in biology from Northern State University, Aberdeen, SD, and the M.S. degree in environmental science from the School of Public and Environmental Affairs, Indiana University, Bloomington.

He is currently a Research Associate at the Center for Agriculture, Resource, and Environmental Systems, University of Missouri-Columbia. His research focuses on environmental management and remote sensing for natural resource planning.